Preparation, Structural And Optical Characterization of Fe_2O_3 Thin Film By SILAR Method

V. Annalakshmi[1], K. Kasirajan[2], S. Maheswari[3], M. Karunakaran[4], C.Subbu[5]
[1, 2, 3, 4, 5] Dept of Physics
[1, 2, 4, 5] Alagappa Government Arts College, Karaikudi – 630 003, India
[3]Caussanel College of Arts and Science,
Muthupettai - 623 523, India.

Abstract- *Thin film of Fe_2O_3 with thickness of 1.2 µm was deposited by successive ionic layer adsorption and reaction (SILAR) method onto glass substrates using ferrous sulphate and sodium hydroxide as cationic and anionic precursors. The X-ray diffraction studies revealed that, a- Fe_2O_3 thin film was polycrystalline in nature with cubic structure. The morphological property was investigated by field emission scanning electron and atomic force microscopy. The optical studies have been carried out by using UV-Vis spectrophotometer to determine the band gap of prepared film.*

Keywords- Thin film, XRD, SILAR, UV-Vis Spectrophotometer, band gap.

I. INTRODUCTION

The researchers are extensively investigating simple and economic deposition techniques to grow metal oxide materials which are suitable substitute for the existing semiconductors [1]. Amongst various metal oxides, iron oxide (α-Fe2O3) is a thermodynamically stable oxide of hexagonal close packed crystal structure with indirect and direct band gap energies around 1.9 and 2.7 eV, respectively [2]. In recent years, much attention of scientific community has been focused on iron oxides due to their potential applications such as magnetic devices [3], gas sensor [4-7], solid state lithium ion battery [8], super capacitor [9], humidity sensor [10], water splitting for hydrogen production [11], solar cell [12, 13], solar filters [14] etc. Apart from this iron oxide nanostructures are technologically important due to their possible applications in many fields including high density magnetic storage devices, magnetic refrigeration systems, catalysis and chemical and biological sensors [15, 16]. In addition to this recently iron oxide has became a novel material for its potential applications in medical science such as drug delivery system, cancer therapy and magnetic resonance imaging due to its biocompatibility, catalytic activity and low toxicity [17–19]. A variety of chemical techniques have been used to fabricate iron oxide thin films such as spray pyrolysis [20, 21], thermal decomposition [22], atomic layer deposition [6], electrodeposition [23], ion-beam assisted deposition [24], RF magnetron sputtering process [25], chemical vapor deposition [26, 27] and SILAR method [28] etc. Among them, SILAR is simple, practical, nonhazardous and low cost soft chemical method. In SILAR technique, nanocrystalline thin films are grown by immersing substrate into separately placed cationic and anionic precursors. In between each immersion substrates are rinsed with purified water, so that only tightly adsorbed layer of species stays on the substrate. In the present work, SILAR method has been developed to grow device quality nanocrystalline iron oxide thin films onto glass substrates as no significant data was published on optical, structural and electrical properties of α-Fe2O3 films.

II. MATERIALS AND METHODS

(i) Experimental Details:

Fe_2O_3 thin film was prepared by SILAR method on a glass substrate at room temperature. For the deposition of Fe_2O_3 thin films, 0.025M ferrous sulphate was used as the cationic precursor solution and anionic precursor solution was 0.1M sodium hydroxide. Before actual deposition glass substrates were boiled in chromic acid, washed with soap solution and finally cleaned with HCl and de-ionized water to provide clean substrate surface to achieve uniform deposition. The well cleaned glass substrate was immersed in a cationic precursor solution ($FeSO_4$) for 10s for the adsorption of iron species on the substrate surface. The substrate was rinsed in double distilled water for 5s to remove loosely bound species of Fe^{2+} species. Then, the substrate was immersed in anionic precursor solution (NaOH) which was kept at 200K for 15s to form a layer of iron oxide material. Rinsing the substrate again in double distilled water for 5s separates out the excess or unreached species. Thus one SILAR cycle of Fe_2O_3 deposition was completed. 120 such deposition cycles were repeated at room temperature (300 K) to get a terminal thickness. The maximum thickness obtained for Fe_2O_3 thin film was 1.2 µm and used for the further. The deposited film was annealed 200^0

C for 1hr to reddish colored pure Fe_2O_3 thin film. The four beaker SILAR mechanism is shown in figure 1.

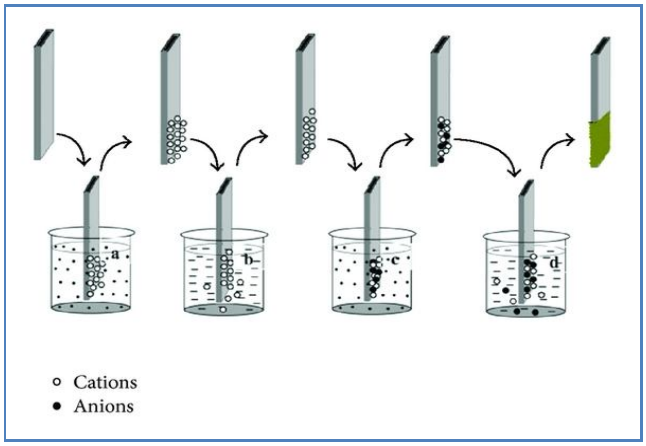

Figure 1: SILAR mechanism:
(a) Cationic Precursor (b) & (d) hot water and (c) anionic precursor

(ii) Characterization Techniques:

The structure and phase of the prepared sample was determined by X-ray diffraction (XRD) using P-Analytical X-ray diffractometer using Cu-Kα (λ=1.540 Å) radiation. Diffraction patterns had been recorded over the 2θ range of 10^o to 80^o at the scan rate of 2^o per minute. The surface morphology and elemental analysis of the synthesized samples were studied by FEI Quanta 250 field emission scanning electron microscope (FESEM). The optical absorbance spectra for the synthesized samples were recorded using UV-vis spectrophotometer (Perkin-Elmer Lamda 35) in the wavelength range of 190 nm - 1100 nm.

III. RESULTS AND DISCUSSION

(i) Micro-structural analysis:

The crystalline structure of the synthesized sample was recorded with the X-ray diffraction using Cu-Kα radiation (λ=1.540 Å). The intensity data were collected over a 2θ range of 10^o - 80^o. The XRD pattern of as the synthesized Fe_2O_3 thin film was shown in figure 2. The patterns indicate that the prepared Fe_2O_3 film consistent with a cubic structure which are in close agreement with the standard JCPDS card number 39-1346. From the XRD patterns, the most prominent peak observed in the figure corresponds to the lattice plane of (110). Other peaks corresponding to the lattice plane (111), (211), (310), (330), (442) and (554) were observed with varying intensities.

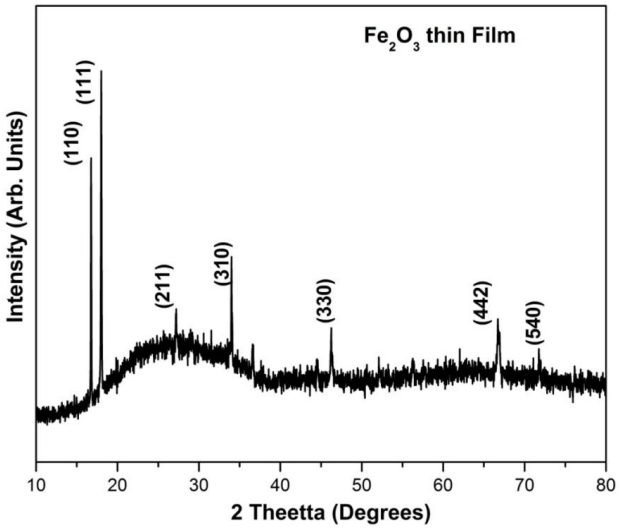

Figure 2: XRD pattern of Fe_2O_3 thin film

The crystallite size of the prepared sample is calculated from the Debye-Scherer's formula. Let λ be the wavelength of X-rays used and β and θ are full width at half maximum and Bragg's angles corresponding to the maximum intensity peak. The Debye-Scherer's (DS) formula [29] is given as,

$$D = \frac{k\lambda}{\beta Cos\theta}$$

According to uniform deformation model, we consider the prepared material is isotopic in nature and the strain is assumed to be uniform in all crystallographic direction. The Williamson-Hall equation according to UDM is given by [30]

$$\beta_{hkl}\cos\theta_{hkl} = \frac{K\lambda}{D} + 4\varepsilon \sin\theta_{hkl}$$

Dislocations an imperfection in crystal associated with the misregistry of lattice existing in different parts of the crystal. Dislocation density (δ) was evaluated using the relation [29]

$$\delta = \frac{1}{D^2}$$

The strain (ε) is calculated from the following relation

$$\varepsilon = \frac{\beta\cos\theta}{4}$$

The X-ray diffraction peak of films corresponding texture coefficient (T_C) is estimated using an expression [30]

$$T_c(h_i k_i l_i) = \frac{I(h_i k_i l_i)}{I_0(h_i k_i l_i)} \left[\frac{1}{n} \Sigma \frac{I(h_i k_i l_i)}{I_0(h_i k_i l_i)} \right]^{-1}$$

where I_0 represents the standard intensity, I is the observed intensity of $(h_i k_i l_i)$ plane and n is the reflection number.

Table 1: Micro- structural parameters of Fe_2O_3 Thin film

Micro-structural properties	Fe_2O_3 Thin film
Crystallite Size using Debye- Scherer's formula (nm)	95.284
Crystallite Size using Williamson-Hall equation (nm)	122.508
Dislocation Density (δ) X 10^{14} / m^2	1.101
Strain (ε) X 10^{-3}	2.060
Texture coefficient	1.248

(ii) Morphological analysis:

The SEM photographs provide the nature of the surface (i.e) uniformity, smoothness and cracks, the nature of the grains (i.e) shape of particulate and grain size. A large number of scanning probe microscopy techniques utilizing various signals generation mechanism has emerged recent years scanning tunneling microscopy is the most important technique with the wide range of applications in science and technology. In this study, the surface morphology of Fe_2O_3 was carried out using SEM and is discussed.

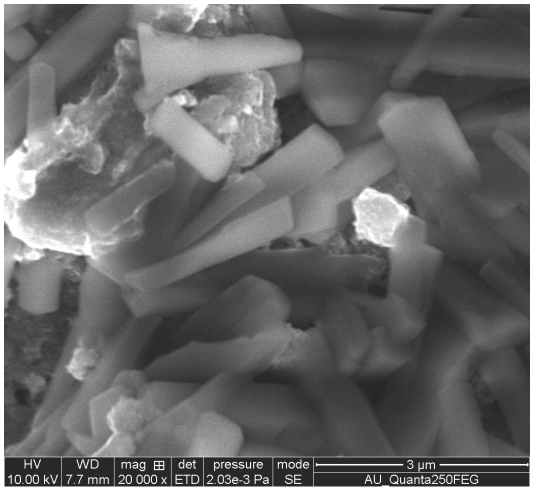

Figure 3 (a): SEM images of Fe_2O_3 Thin film (3 µm)

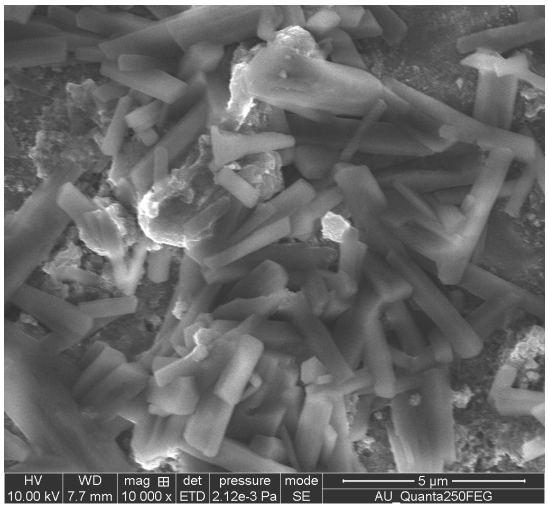

Figure 3 (b): SEM images of Fe_2O_3 Thin film (5 µm)

The surface morphology of the iron oxide thin films deposited onto glass substrates by SILAR method was examined using FESEM. Figure 3 (a) and (b) are shown the SEM micrograph of Fe_2O_3 for 3µm and 5µm magnification respectively. It is observed that, the a-Fe2O3 rod shaped grains are distributed and covers whole substrate surface and found that there is no uniform shape. In some places, various sizes of the particles (small and large size) are observed, i.e. rod shaped particles seem to be randomly distributed. Such image is compact and relatively not dense. This is because smaller primary particles have a large surface free energy and would, therefore, tend to agglomerate faster and grow into larger grains. This kind of micro structure is desirable for sensor applications.

(iii) Optical analysis

The optical absorption and transmittance measurement of Fe_2O_3 thin film was carried out in the wavelength range from 300 to 1100 nm at room temperature. Figure 4 and 5 shows the optical absorbance transmittance of Fe_2O_3 thin film respectively. It had a maximum absorbance and transmittance in the visible region. Figure 6 shows the variation of $(\alpha h\nu)^2$ with the photon energy for prepared Fe_2O_3 thin film. The optical band gap (Eg) of a- Fe_2O_3 films were estimated by using the relation,

$$\alpha = \frac{A(h\nu - E_g)^n}{h\nu}$$

where a is absorption coefficient; Eg is band gap; A is a constant and n is equal to 1/2 for direct and 2 for indirect transition. From the Tauc's plot, the band gap is found to be 2.52 eV for Fe_2O_3 thin film, which is in good agreement with the previous results (2.9 eV) [31].

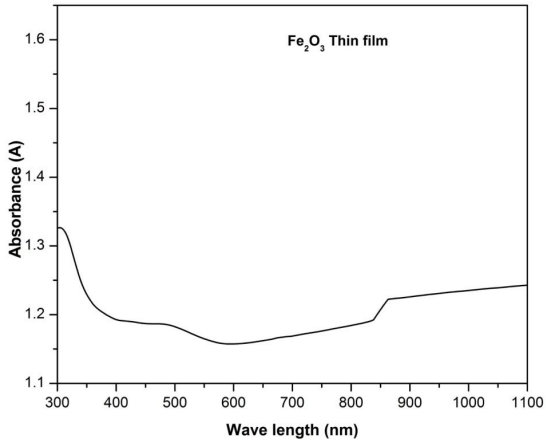

Figure 4: Optical absorbance spectra of Fe_2O_3 thin film

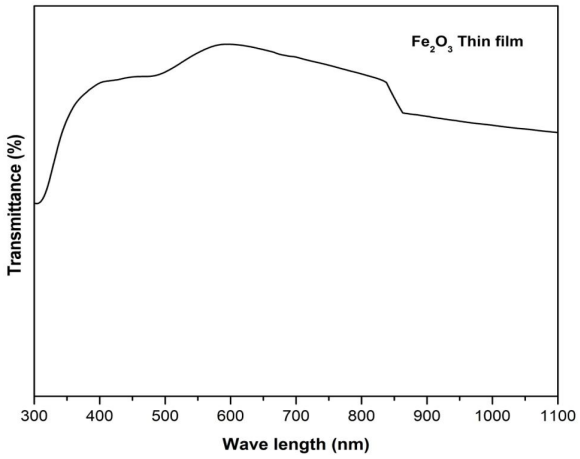

Figure 5: Optical transmission spectra of Fe_2O_3 thin film

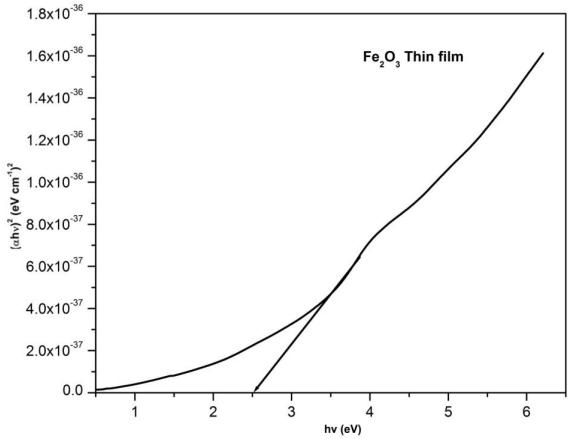

Figure 6: Tauc's plot of Fe_2O_3 Thin film

IV. CONCLUSION

Fe_2O_3 thin film was successfully prepared by cost effective SILAR method. The X-ray diffraction pattern indicates that, the prepared Fe_2O_3 thin film is cubic structure with poly crystalline in nature. The microstructural parameters were estimated. The crystallite size of the sample was calculated using Scherer's equation and Williamson-Hall equation. A SEM result of prepared film has rod shaped morphology throughout the surface. UV vis results indicates the prepared sample have good absorption and transmittance values in visible region. The calculated direct band gap of energy was 2.52 eV for prepared samples.

REFERENCES

[1] M. R. Belkhedkar, A. U. Ubale "Preparation and Characterization of Nanocrystalline α-Fe2O3 Thin Films Grown by Successive Ionic Layer Adsorption and Reaction Method", International Journal of Materials and Chemistry, 4(5): 109-116, 2014.

[2] J. A. Glasscock, P. R. F. Barnes, I. C. Plumb, A. Bendavid, P. J. Martin, "Structural, optical and electrical properties of undoped polycrystalline hematite thin films produced using filtered arc deposition", Thin Solid Films, vol.516, pp.1716, 2008.

[3] J. Mallinson, The Foundations of Magnetic Recording, second ed., Academic Press, New York, 1993.

[4] S. Wang, W. Wang, W. Wang, Z. Jiao, J. Liu, Y. Qian, "Characterization and gas-sensing properties of nano-crystalline iron_III/oxide films prepared by ultrasonic spray pyrolysis on silicon", Sens. Actuators B vol.69, pp. 22, 2000.

[5] S. Wang, L. Wang et al., "Porous α-Fe2O3 hollow microspheres and their application for acetone sensor", J. Solid State Chem., vol. 183, pp. 2869, 2010.

[6] D. Patil, V. Patil, P. Patil, "Highly sensitive and selective LPG sensor based on α-Fe2O3 nanorods", Sens. Actu. B, vol. 152, pp. 299, 2011.

[7] M. Aronniemi, J. Saino, J. Lahtinen, "Characterization and gas-sensing behavior of an iron oxide thin film prepared by atomic layer deposition" Thin Solid Films, vol. 516, pp. 6110, 2008.

[8] H. Kitaura, K. Takahashi, F. Mizuno, A. Hayashi, K. Tadanaga, M. Tatsumisago, "Mechanochemical synthesis of α-Fe2O3 nanoparticles and their application to all-solid-state lithium batteries", J. Power Sources, vol. 183, pp.418, 2008.

[9] P. M. Kulal, D. P. Dubal, C. D. Lokhande, V. J. Fulari, "Chemical synthesis of Fe2O3 thin films for supercapacitor application", J. Alloys Comp., vol. 509, pp. 2567, 2011.

[10] M. Pelino, C. Colella, C. Cantalini, M. Faccio, G. Ferri, A. D'Amico, "Microstructure and electrical properties of an C–hematite ceramic humidity sensor", Sens. Actuators B, vol.7, pp. 464, 1992.

[11] M. Frites, Y. A. Shaban, S. U.M. Khan, "Iron oxide (n-Fe2O3) nanowire films and carbon modified (CM)-n-

Fe2O3 thin films for hydrogen production by photosplitting of water" Int. J. hydrogen energy, vol. 35, vol. 4944, 2010.

[12] J. H. Kennedy, D. J. Dunnwald, "Photooxidation of organic compounds at α-Fe2O3 electrodes", Electro-chem. Soc., vol. 130, pp. 2013, 1983.

[13] J. S. Im, S. K. Lee, Y. S. Lee, "Cocktail effect of Fe2O3 and TiO2 semiconductors for a high performance dye-sensitized solar cell", Appl. Surf. Sci., vol. 257, pp. 2164, 2011.

[14] J. C. Galan, R. Almanza, "Solar filters based on iron oxides used as efficient windows for energy savings", Solar Energy, vol. 81, pp. 13, 2007.

[15] V. Sreeja, P. A. Joy," Microwave–hydrothermal synthesis of γ-Fe2O3 nanoparticles and their magnetic proper- ties", Mater. Res. Bull., vol. 42, pp. 1570, 2007.

[16] J. Du, H. Liu, "Preparation of super paramagnetic γ-Fe2O3 nanoparticles in nonaqueous medium by γ - irradiation" J. Magn. Magn. Mater., vol. 302, pp. 263, 2006.

[17] X. Jing, Y. Haibin, F. Wuyou, D. Kai, Y. Sui, J. Chen, Y. Zeng, M. Li, G. Zou, J. Magn. Magn. Mater., vol. 309, pp. 307, 2007.

[18] B. Fang, G. Wang, W. Zhang, M. Li, X. Kan, "Fabrication of Fe3O4 nanoparticles modified electrode and its application for voltammetric sensing of dopamine", Electroanalysis, vol. 17, pp.744, 2005.

[19] A.K. Gupta, M. Gupta, "Synthesis and surface engineering of iron oxide nanoparticles for biomedical applications", Biomater., vol. 26, pp. 3995, 2005.

[20] R. N. Goyal, D. Kaur, A. K. Pandey, "Growth and characterization of iron oxide nanocrystalline thin films via low-cost ultrasonic spray pyrolysis", Mater. Chem. Phys., vol.116, pp. 638, 2009.

[21] A. A. Akl, "Microstructure and electrical properties of iron oxide thin films deposited by spray pyrolysis" Appl. Surf. Sci., vol. 221, pp. 319, 2004.

[22] J. Hua, Y. Heqing, "Thermal decomposition synthesis of 3D urchin-like α-Fe2O3 superstructures", Mater. Sci. Engg. B., vol. 156, pp. 68, 2009.

[23] S. S. Kulkarni, C. D. Lokhande, "Structural, optical, electrical and dielectrical properties of electrosynth-sized nanocrystalline iron oxide thin films", Mater. Chem. Phys., vol.82, pp. 151, 2003.

[24] Y. J. Park, K. M. A. Sobahan, C. K. Hwangbo, "Optical and structural properties of Fe2O3 thin films prepared by ion-beam assisted deposition", Surf. Coat. Technol., vol. 203, pp. 2646, 2009.

[25] J. D. Uribe, J. Osorio, C. A. Barrero, D. Girata, A. L. Morales, A. Hoffmann, "Physical properties in thin films of iron oxides", J. Microelectro., vol. 39, pp.1391, 2008.

[26] H. G. Cha, C. W. Kim, Y. H. Kim, M. H. Jung, E. S. Ji, B. K. Das, J. C. Kim, Y. S. Kang, "Preparation and characterization of α-Fe2O3 nanorod-thin film by metal–organic chemical vapor deposition", Thin Solid Films, vol. 517, pp. 1853, 2009.

[27] K. Shalini, G. N. Subbanna, S. Chandrasekaran, S. A. Shivashankar, "Thin films of iron oxide by low presure MOCVD using a novel precursor: tris (t-butyl-3-oxobutanoato) iron (III)", Thin Solid Films, vol.424, pp. 56, 2003.

[28] S. Park, "Preparation of iron oxides using ammonium iron citrate precursor: Thin films and nanoparticles", J. Solid State Chem., vol. 182, pp. 2456, 2009.

[29] Bruno Chandrasekar, L., Raji, P., Chandramohan, R., Vijayalakshmi, R., Devi, G., Shunmugasundaram, P., Sindhu, P.: J.Nanoelec.Optoelec 8(4), 369 (2013).

[30] Bruno Chandrasekar L., Chandramohan R., Vijayalakshmi R., J. Nanoeng. Nanomanu, 3(3), 253 (2013).

[31] R. Al-Gaashani, S. Radiman, N. Tabet, A.R. Daud, J. Alloy.Compd. 550 (2013) 395-401.